COMPDYN 2013
4th ECCOMAS Thematic Conference on
Computational Methods in Structural Dynamics and Earthquake Engineering
M. Papadrakakis, V. Papadopoulos, V. Plevris (eds.)
Kos Island, Greece, 12–14 June 2013

SEISMIC RESPONSE OF POST-TENSIONED STEEL ROCKING CONCENTRICALLY BRACED FRAMES WITH VARIOUS ASPECT RATIOS

N. Brent Chancellor[1], Richard Sause[1], James M. Ricles[1], Ebrahim Tahmasebi[1], and Tugce Akbas[1]

[1] Lehigh University
117 ATLSS Drive, Bethlehem, PA 18015, USA
{nbc208, rs0c}@lehigh.edu

Keywords: Self-Centering, Rocking, Steel, Concentrically-Braced Frames.

Abstract. *Post-tensioned, steel, rocking concentrically braced frames (also known as self-centering concentrically braced frames or SC-CBFs) are a new type of seismic lateral force resisting system that reduces or eliminates the damage and residual drift often associated with conventional concentrically-braced frames (CBFs) under design level earthquakes. The SC-CBF is made up of a CBF whose column bases are not anchored to the foundation (they are free to uplift), post-tensioning steel that runs vertically over the height of the SC-CBF to prestress the SC-CBF to the foundation and some sort of energy dissipation device. The SC-CBF eliminates the damage to the CBF members under design level earthquakes by limiting the base overturning moment that can develop and then keeping the members nominally elastic. The maximum base overturning moment is limited by allowing the SC-CBF to rock on its foundation and yielding of the post-tensioning steel. The residual drift is reduced or eliminated under design level earthquakes by a prestressing force from the post-tensioning steel running vertically over the height of the SC-CBF. The prestressing force provides a restoring overturning moment that returns the SC-CBF to its original undisplaced state after the earthquake.*

One of the key aspects and assumptions of the SC-CBF system is that the member forces are controlled by limiting the base overturning moment that can develop. Generally, base overturning moment is considered to be a first mode response, but as the aspect ratio increases this assumption becomes less valid. This means that the member forces may not be as well controlled as thought by limiting the base overturning moment. This paper studies the seismic response of six SC-CBFs across a range of aspect ratios through nonlinear time-history analysis and shows how the performance of the SC-CBF changes with aspect ratio.

1 INTRODUCTION

Steel Self-Centering Concentrically-Braced Frames (SC-CBFs) are a new type of seismic lateral force resisting system that are intended to reduce or eliminate the damage and residual drift often associated with conventional concentrically braced frames (CBFs) under the design basis earthquake (DBE) [1, 2]. The SC-CBF system increases the drift capacity of the CBF by allowing the CBF to rock on its foundation. Post-tensioning (PT) bars run vertically over the height of the CBF and provide a restoring overturning moment at the base to self-center the SC-CBF so that there is little or no residual drift. Energy dissipation in an SC-CBF is provided by lateral load bearings with friction at each floor level and/or supplemental energy dissipation devices. Damage to the braces and other members is not a significant energy dissipation mechanism in the SC-CBF, which is in contrast to conventional CBFs which dissipate energy through yielding and buckling of the braces and connecting elements. The hysteretic behavior of the entire SC-CBF seismic lateral force resisting system is characterized by flag shaped hysteresis loops [1]. A schematic of hysteresis loops for an SC-CBF using lateral load bearing with friction for energy dissipation is shown in Figure 1.

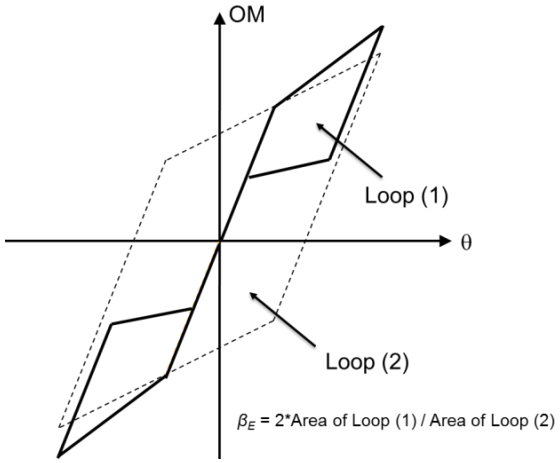

Figure 1: Schematic base overturning moment versus roof drift hysteresis loops for an SC-CBF (Loop 1) and an equivalent bilinear elastic-plastic system (Loop 2). Also shown is a graphical demonstration of the definition of the energy dissipation ratio (β_E).

One of the key aspects and assumptions of the SC-CBF system is that the member forces are controlled by limiting the base overturning moment that can develop. Generally, base overturning moment is considered to be a first mode response, but as the aspect ratio of the SC-CBF increases this assumption becomes less valid. As a result, the member forces may not be controlled as intended by limiting the base overturning moment. This paper studies the seismic response of several SC-CBFs with various heights subjected to design level earthquakes. First the SC-CBF system and its behavior are outlined. Then the designs of the archetype SC-CBFs studied in this paper are described. Details of the numerical model used in time-history analyses are given, followed by details about the ground motion set used in time-history analyses. Results from the time-history analyses are described. Finally, the behavior of the archetype SC-CBFs at various aspect ratios is studied to show how the performance of the SC-CBF system changes with aspect ratio.

2 SC-CBF SYSTEM AND BEHAVIOR

An SC-CBF is similar to a conventional CBF in that it is made up of beams, columns and braces connected together in such a manner that the applied external forces are resisted primarily through axial forces in the members. However, a few changes to the conventional CBF provide the SC-CBF with larger drift capacity and self-centering behavior after a significant earthquake [1, 2]. The first significant change is that the SC-CBF column bases are not vertically anchored to the foundation; they are free to uplift and allow the SC-CBF to rock at its base during the earthquake. The SC-CBF is restrained in the horizontal direction at the base level. The SC-CBF has post-tensioning (PT) steel which runs vertically over the height of the SC-CBF. This PT steel is prestressed and clamps the SC-CBF to its foundation. The purpose of the PT steel is to provide an initial base overturning moment resistance as well as a restoring base overturning moment so that the SC-CBF will return to its plumb condition. A third difference is that the SC-CBF system includes an extra gravity column adjacent to each SC-CBF column. This extra gravity column allows the floor diaphragm to be separated from the SC-CBF so that it will not be damaged when the SC-CBF columns uplift during an earthquake. A lateral load bearing is located between the SC-CBF column and the adjacent gravity column. The lateral load bearing transfers the lateral forces from the floor diaphragm (attached to the gravity column) to the SC-CBF while still allowing the SC-CBF columns to uplift, preventing floor diaphragm damage. The lateral load bearings also act as passive energy dissipation devices due to the normal force and frictional force that develops in the bearing from the lateral loads and the relative vertical motion between the SC-CBF column and the adjacent gravity column. An SC-CBF also includes a horizontal base strut between the bases of the SC-CBF columns to transfer base shear from the uplifted SC-CBF column to the SC-CBF column in contact with the foundation. A vertical "distribution" strut in the upper stories of the SC-CBF at the center of the bay is included to distribute the large vertical force from the PT steel to braces in the upper stories of the SC-CBF. A typical SC-CBF with adjacent gravity columns and lateral load bearings with friction is shown in Figure 2a.

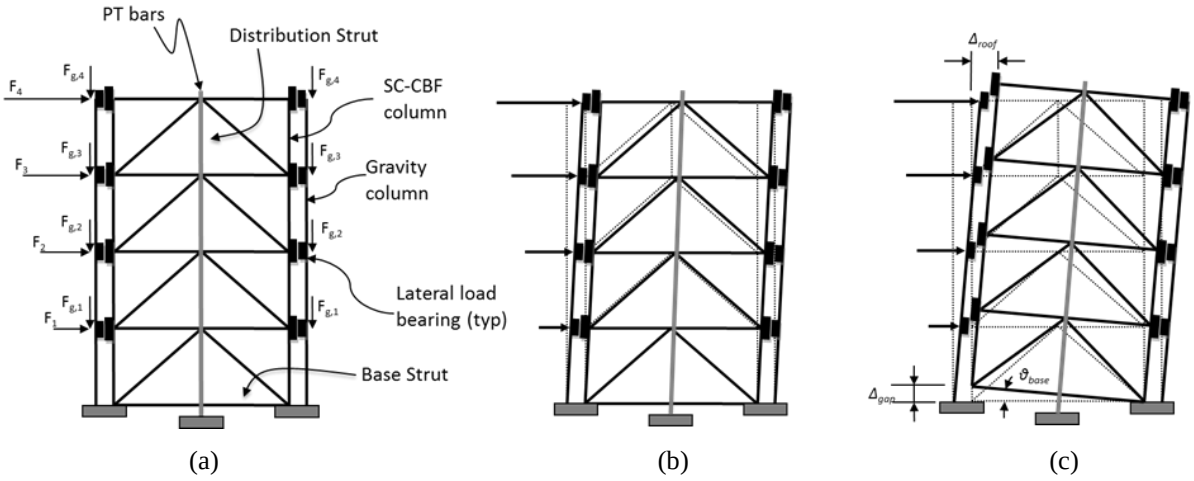

Figure 2: Lateral load behavior of SC-CBF: (a) layout of typical SC-CBF with gravity and lateral forces; (b) elastic response of SC-CBF frame before SC-CBF "tension" column decompresses and lifts up; (c) rigid body rocking of frame on foundation.

As lateral force is applied to the SC-CBF (shown in Figure 2a) the SC-CBF will deform elastically (Figure 2b) similar to a conventional CBF. However, after the applied base overturning moment becomes large enough to overcome the initial overturning moment resistance

provided by the prestress force in the PT bars, the SC-CBF weight and the friction in the lateral load bearings, one column will uplift or "decompress" and the SC-CBF will begin to rock on its foundation (Figure 2c). As the lateral force is reduced, the force in the PT bars provides a restoring overturning moment to return the SC-CBF to its plumb, upright position.

The internal forces that can develop in the members of the SC-CBF are intended to be limited by the rocking action of the SC-CBF (and yielding of the PT bars if the lateral drift demand is large enough). After decompression, the stiffness of the SC-CBF system is primarily controlled by the area and location of the PT bars.

An experimental study of a 4-story, 0.6 scale SC-CBF was performed at Lehigh University to validate the SC-CBF lateral force resisting system concept. The results of this study are covered extensively in references [2, 3, 4]. The testing program used the hybrid simulation technique [5] and simulations were performed pseudo-dynamically. Simulations were performed at the DBE and maximum considered earthquake (MCE) demand levels. Thirty one successful simulations were performed showing that large ductility without damage or residual drift can be achieved for SC-CBFs.

Most studies of the SC-CBF concept or variants of the concept are limited to structures 6-stories or less in height [1, 2, 6, 7, 8, 9, 10]. This paper addresses the behavior of SC-CBFs at many aspect ratios, including structures up to 18 stories.

3 DESIGN OF ARCHETYPE SC-CBF STRUCTURES

3.1 Floor Plan and Elevation Layouts

All of the archetype SC-CBFs studied in this paper were designed using a performance-based design procedure from reference [1] with a few modifications. Schematics for the floor plan and elevation layouts for the archetype SC-CBFs structures studied in this paper are shown in Figure 3. The structure is symmetric in two directions and eight SC-CBFs are distributed around the perimeter of the structure. This symmetry requires only a single SC-CBF for each structure to be designed.

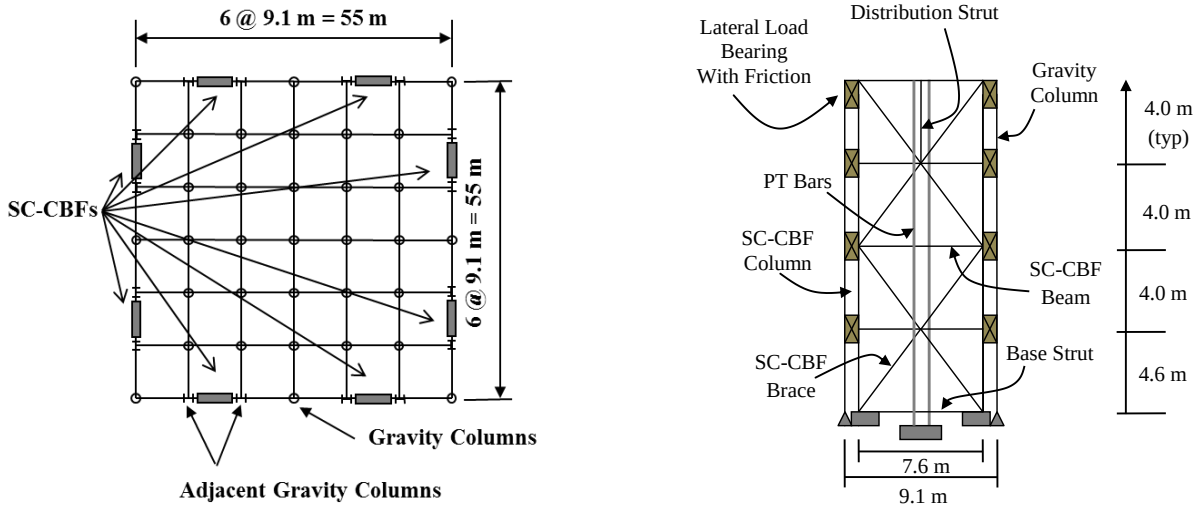

Figure 2: Lateral load behavior of SC-CBF: (a) layout of typical SC-CBF with gravity and lateral forces; (b) elastic response of SC-CBF frame before SC-CBF "tension" column decompresses and lifts up; (c) rigid body rocking of frame on foundation.

The braces of the archetype SC-CBFs studied in this paper are arranged in an x-braced configuration. A gravity column is located adjacent to each SC-CBF column. High strength, high ductility post-tensioning (PT) bars run vertically over the height of the SC-CBF at mid-bay. A vertical distribution strut is located at the center of the bay in the top one or two stories to distribute the large concentrated force from the PT bars to the braces in the top two or three stories. A horizontal base strut is located at the bottom of the SC-CBF between the SC-CBF columns to transfer base shear from the uplifted column to the column in contact with the foundation.

3.2 Loads on Archetype SC-CBFs

The dead loads for the archetype SC-CBF structures are expressed in terms of a floor pressure and are shown in Table 1. The live loads for the archetype SC-CBF structures are expressed as a floor pressure in Table 2. The structures are assumed to be office-type structures. Wind loads and other loading conditions were not considered in the design of the archetype SC-CBFs.

Dead Load (kN/m^2)	Floor 1	Middle Floors	Roof
Floor/Roof Deck	0.14	0.14	0.14
Floor/Roof Slab	2.06	2.06	0
Roofing Material	0	0	0.48
Mechanical Weight	0.48	0.48	1.20
Ceiling Material	0.24	0.24	0.24
Floor Finish	0.10	0.10	0
Structural Steel	0.72	0.72	0.48
Steel Fireproofing	0.10	0.10	0.10
Building Envelope	0.37	0.35	0.25
Total	**4.20**	**4.18**	**2.89**

Table 1: Summary of dead loads.

Live Load (kN/m^2)	Floors	Roof
Office	2.39	0
Partitions	0.72	0
Roof (unreduced)	0	0.96
Total	**3.11**	**0.96**
Live Load Included in Seismic Mass	0.72	0

Table 2: Summary of live loads.

3.3 Archetype SC-CBF Designs

All of the SC-CBF members were designed using wide-flange shapes that meet the seismic compactness requirements of ANSI/AISC 341-05 [11]. The specified yield strength of the steel for the SC-CBF and CBF members was 0.35 kN/mm^2 and the modulus of elasticity was 200 kN/mm^2. The yield strength for the PT bars for the SC-CBF was assumed to be 0.83 kN/mm^2 and the modulus of elasticity was assumed to be 205 kN/mm^2.

The seismic design category for the SC-CBF and CBF was Category D [12]. The short period spectral acceleration used in design (S_S) was 1.5g and the 1 sec period spectral acceleration used in design (S_1) was 0.6g. The site class was assumed to be Site Class D [12].

Six archetype SC-CBFs were designed (4, 6, 9, 12, 15, and 18-stories). Table 4 lists important parameters for each archetype SC-CBF design. The aspect ratio is the height of the archetype SC-CBF divided by the width of the SC-CBF, T_1 is the first mode period of the SC-CBF calculated using a fixed base linear numerical model, θ_{DBE} is the predicted roof drift un-

der the DBE, β_E is the energy dissipation ratio (ratio of the area of idealized SC-CBF hysteresis loops to an equivalent bilinear elastic plastic system, see Figure 1), β_{SC} is a measure of the self-centering capability of the archetype SC-CBF (β_{SC} must be less than 0.50 to ensure self-centering behavior), and R_A is similar to the response modification coefficient, *R*, used in building codes for seismic design of structures and will be explained further later. Table 4 also lists the parameters that strongly influenced the design of the archetype SC-CBFs. *AMS* indicates that the available member sizes influenced the design of the archetype SC-CBF, and θ_{DBE} indicates that drift influenced the design. Some archetype SC-CBF designs required members larger than the typical column sections listed in the 13th Edition of the AISC Steel Construction Manual [13].

The aspect ratio for the archetype SC-CBFs varies from approximately 2 for the 4-story SC-CBF to approximately 10 for the 18-story. The first mode period varies from 0.48 sec to 3.30 sec. The predicted roof drift (θ_{DBE}) is approximately 1.5% radians for most of the archetype SC-CBFs. The roof drift values are calculated using ductility-response modification coefficient-period (μ-*R*-*T*) relationships developed by Seo [14] for self-centering systems.

The energy dissipation ratio (β_E) decreases with increasing aspect ratio, but the lateral load bearings still allow the SC-CBF columns to uplift without damaging the floor system. Additional energy dissipation devices, such as yielding elements, can be added to increase β_E, but were not used for the archetype SC-CBFs studied in this paper. Additional energy dissipation can reduce the required amount of PT steel, which in turn will reduce the SC-CBF member sizes. β_{SC} for the archetype SC-CBFs was intentionally kept below 0.50 to ensure that the SC-CBFs will self-center. If β_{SC} is greater than 0.50, the hysteresis loops for the SC-CBF will extend into the second and fourth quadrants on a plot of the hysteresis loops and self-centering is not guaranteed.

Archetype	**Aspect Ratio (height/width)**	***T_1 (sec)***	***θ_{DBE}* (% rad)**	***β_E***	***β_{SC}***	***R_A***	***SC-CBF Weight (kN)***	***Parameter Controlling Design***
4-story	2.16	0.48	1.02	0.51	0.35	7.45	205	-----
6-story	3.20	0.84	1.51	0.36	0.23	13.2	326	θ_{DBE}
9-story	4.76	1.32	1.52	0.20	0.16	12.7	700	θ_{DBE}
12-story	6.32	1.78	1.51	0.14	0.12	10.2	1236	θ_{DBE}
15-story	7.88	2.39	1.51	0.11	0.096	7.84	1992	θ_{DBE},*AMS**
18-story	9.44	3.30	1.66	0.086	0.080	5.82	2760	θ_{DBE},*AMS**

Table 3: Summary of design parameters for archetype SC-CBFs.

R_A is a parameter similar to the response modification coefficient, *R*, in ASCE 7-05 (ASCE 2005) and ASCE 7-10 (ASCE 2010). R_A is calculated as follows:

$$R_A = \frac{OM_{elastic}}{OM_D} \tag{1}$$

where, $OM_{elastic}$ is the base overturning moment calculated using the equivalent lateral forces from ASCE 7 with R=1 and OM_D is the overturning moment when the SC-CBF uplifts and rocking begins. The calculation of OM_D is explained further in Roke et al. [2]. The values of $OM_{elastic}$ and OM_D are shown in Table 5 for each archetype SC-CBF studied in this paper. Also in Table 5 are the base overturning moment at yield of the PT steel and the peak overturning moment predicted for the design basis earthquake, which is based on estimated drift.

The area of PT steel used in each archetype SC-CBF design along with the initial prestress ratio (initial prestress force/yield force) is summarized in Table 5. The amount of PT steel

can be reduced if added energy dissipation devices are used, because additional PT steel is used to help control the "*R*" parameter used to predict the drift demand. Increasing OM_D reduces the "*R*" parameter used in the drift prediction and reduces the expected roof drift under the DBE (θ_{DBE}). Added energy dissipation devices also increase β_E, which also reduces θ_{DBE}.

Archetype	Area of PT Steel (cm^2)	Initial Prestress Ratio (% of Yield Force)	OM_D (MN-m)	OM_Y (MN-m)	$OM_{elastic}$ (MN-m)	OM_{DBE} (MN-m)
4-story	81	0.50	20.6	40.0	153.6	40.6
6-story	102	0.47	21.3	43.5	281.6	43.6
9-story	169	0.55	37.9	66.4	480.4	60.4
12-story	237	0.75	68.7	89.9	703.1	90.4
15-story	403	0.80	120.6	148.7	945.3	146.9
18-story	671	0.85	206.8	241.3	1205	236.8

Table 4: Summary of additional design parameters for archetype SC-CBFs.

A key assumption about the behavior of an SC-CBF under earthquake load is that the base overturning moment is primarily a first mode response and that rocking behavior of the SC-CBF will limit the overturning moment that can develop. If this assumption is violated, the braces and other members of the SC-CBF must be designed for larger forces or, damage to the members must be accepted by the performance criteria. To assess the contributions of each mode to the base overturning moment, the modal overturning moment at the base of the archetype SC-CBFs were calculated and then normalized by dividing by the sum of the absolute values of the modal base overturning moments for all of the modes. The contribution of the modal base overturning moment for the first two modes to the sum of the absolute value of the base overturning moment for all of the modes is shown in Figure 4.

In Figure 4, as the number of stories increases up to 12-stories, the normalized first mode base overturning moment decreases rapidly while the normalized second mode overturning moment increases rapidly. The first mode and second mode base overturning moment are about the same for the 12, 15, and 18-story archetypes. Figure 4 indicates that the SC-CBF system may be more effective for structures with fewer stories or smaller aspect ratios. The results from time-history analyses of the archetype SC-CBFs will be used to study this issue further.

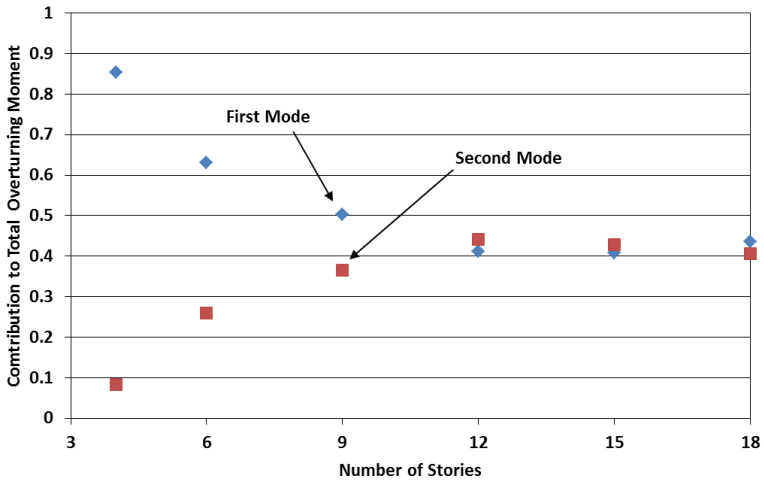

Figure 4: Plot of modal overturning moment contributions for the 4, 6, 9, 12, 15, and 18-story SC-CBFs.

4 EVALUATION OF ARCHETYPE SC-CBFS USING TIME-HISTORY ANALYSES

4.1 Modeling of Archetype SC-CBFs for Time-History Analyses

Nonlinear numerical models for the archetype SC-CBFs were created in OpenSees [15]. OpenSees is an open source nonlinear dynamic analysis software package. The numerical model was a two dimensional (planar) model. The braces in the numerical model form an "x" configuration with the bottom end of the first story braces attaching to the columns. A schematic of the numerical model is shown in Figure 5. There is a gravity column located adjacent to each SC-CBF column. A lean-on column is connected to the adjacent gravity columns and models the gravity system tributary to the SC-CBF. Lateral load bearings are located at each floor between the SC-CBF columns and the adjacent gravity columns.

All of the archetype SC-CBF members are modeled using beam-column elements with an elastic material model. An elastic material model was used because the design procedure intends to keep the members elastic under DBE level design forces. The nonlinearity in the SC-CBF is expected to be from rocking action and yielding of the PT steel. The lateral load bearings are modeled using a friction-contact-gap element. The friction-contact-gap element models friction behavior using a slightly modified Mohr-Coulomb friction model to account for the contact and friction stiffness. A small, initial gap in the lateral load bearings is modeled.

The steel post-tensioning (PT) bars used in the design of the archetype SC-CBFs are represented in the numerical models by a beam-column element with section and material properties such that the total axial yield force of the PT bars is the same as that in the model. The material model for the PT bars was bilinear elastic-plastic with a 2% post-yield slope. The yield strength of the PT bars was modeled as 0.83 kN/mm^2. The PT bars in the numerical model are anchored at a node located at the center of the SC-CBF at the roof level and at a node 0.91 m below the base level. The 0.91 m of PT bar length below the base level is intended to represent the additional free length of PT bar that would be present in the anchorage in the foundation. At the node where the PT steel is anchored there is a zero-length element. The zero-length element is used to modify the PT steel model so that the PT steel can only carry tension loads and allow for "slack" or gap condition to form at the base of the PT bars if the permanent deformation in the PT bars becomes large enough.

The model has six locations where boundary conditions are applied. These locations include: the base of the lean-on column, the base of each gravity column adjacent to the SC-CBF columns, the base of each SC-CBF column, and one location at the anchorage of the PT bars. The boundary condition at the base of the lean-on column is a "pin" condition where the vertical and horizontal displacement are restrained, but the rotation is not. The base of each gravity column (adjacent to the SC-CBF columns) has a pinned condition. The boundary condition at the base of each SC-CBF column models the vertical and horizontal gap and contact condition. Two zero-length elements are used at each SC-CBF column base. One zero-length element models the vertical gap and contact condition while the other zero-length element models the horizontal gap and contact condition. The material/behavior model for the zero length elements at the SC-CBF column base has a positive stiffness as the column is displaced towards the foundation while the stiffness in the other direction is very small, creating a linear elastic-gap model. The element that connects the zero-length element at the base of the PT bars to the foundation is restrained so that only axial deformation is possible. Figure 6 shows a schematic of the boundary conditions of numerical model.

The lateral degree-of-freedom at each floor of the gravity columns (adjacent to the SC-CBF columns) is constrained to the lean-on column in the numerical model. The seismic

mass at each floor level is assigned to the horizontal degree of freedom at the lean-on column node at each respective floor level. In addition to the seismic mass applied to the lean-on column a small mass was applied to the center node of the SC-CBF or CBF at each floor. This mass was applied for numerical stability of the SC-CBF numerical model. The sum of the masses applied to the center of the SC-CBF equals the total mass of the SC-CBF. The mass at the center nodes of the SC-CBF was assigned to both the vertical and horizontal degrees-of-freedom since the SC-CBF floor center nodes may have both significant lateral and vertical motion.

Second order effects are considered in the numerical model through use of a lean-on column and a corotational geometric transformation. Inherent damping in the structure was modeled using Rayleigh damping with 2.6% damping in the first mode and 6.1% in the third mode.

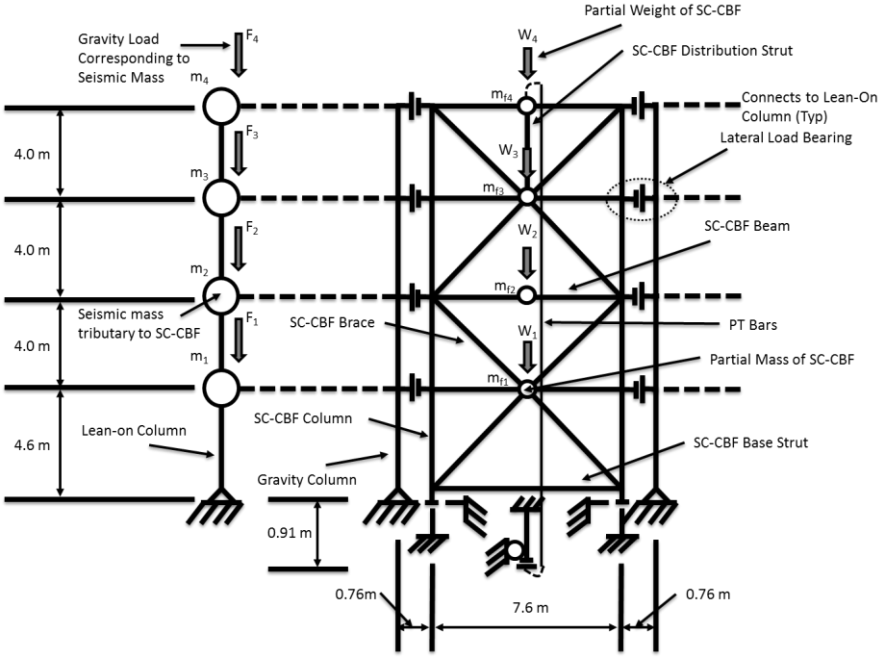

Figure 5: Schematic of numerical model layout for archetype SC-CBFs.

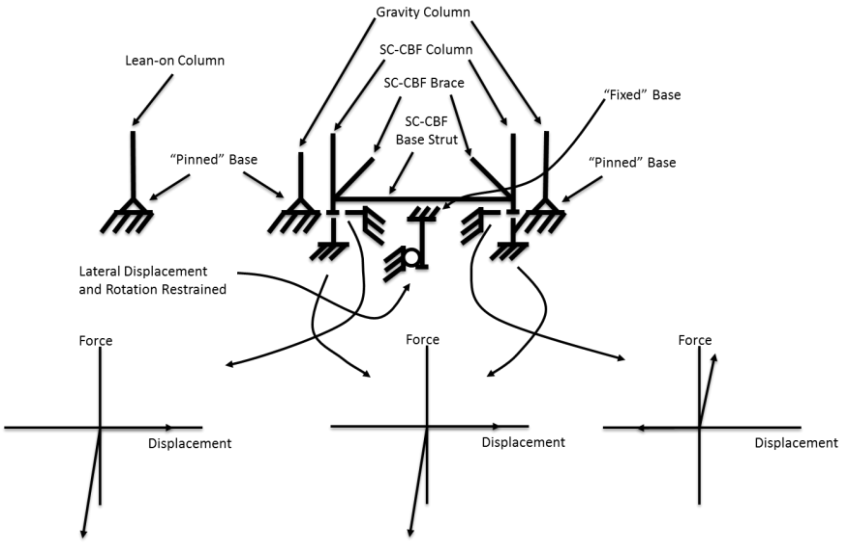

Figure 6: Numerical model boundary conditions for archetype SC-CBFs.

4.2 Ground Motions Used in Study of Archetype SC-CBF Structures

The ground motion set that was used in this study was selected to represent the design spectrum for the archetype SC-BFs over a broad period range. Eighteen ground motion pairs were selected from a subset of the filtered ground motions in the PEER-NGA database [16] meeting some special requirements. Ground motions used in the subset of the PEER-NGA database met the following criteria:

1. The lowest usable frequency of the ground motion was 0.125 Hz or less, providing seismic input to periods of 8 sec or more.
2. The ground motion was recorded on a site with NEHRP Type D soil (based on Vs30).

The eighteen ground motion pairs were selected and scaled to match the design spectrum for the archetype SC-CBFs over the period range of 0.1-7.0 sec. The spectral acceleration and spectral displacement for each scaled ground motion are plotted versus period in Figure 7 along with the design spectrum and the median of the ground motion set. The ground motions were scaled so that the geometric mean of spectral acceleration for the pair of records matched the design spectrum over the period range of 0.1-7.0 sec (with a period increment of 0.01 sec). A scaling method given in Baker [17] was used, which scales each ground motion so that the average spectral acceleration of the target spectrum is equal to the average of the response spectrum over the desired period range. The scale factor calculated using this method is:

$$SF_j = \frac{\sum_{k=1}^{n} SA_{TS}(T_k)}{\sum_{k=1}^{n} SA_{GM}(T_k)} \tag{2}$$

where,

SF_j is the scale factor for ground motion j in the ground motion set
T_k is the k^{th} period in a vector of n periods that will be considered
$SA_{TS}(T_k)$ is the spectral acceleration of the target spectrum at period T_k
$SA_{GM}(T_k)$ is the spectral acceleration of the ground motion being scaled at period T_k.

The scale factor for all ground motion pairs was less than 3.0.

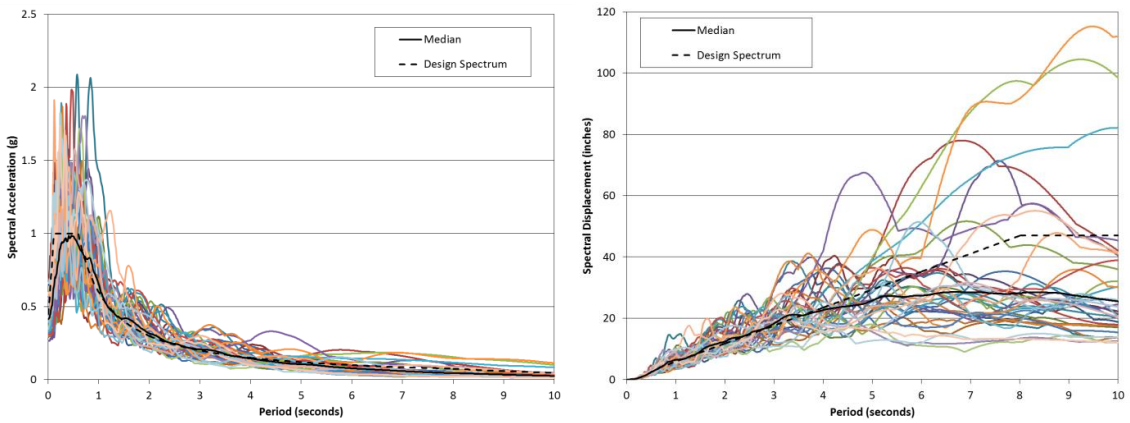

(a) (b)

Figure 7: (a) Spectral acceleration and (b) spectral displacement versus period.

4.3 Results of Time-History Analyses and Seismic Behavior of SC-CBFs

The peak roof drift demand and the peak story drift demand from the time-history analyses of the archetype SC-CBFs are shown in Figure 8. The median value of the peak response is shown with a solid bar. The median peak roof drift on the plot of peak story drifts is shown by an open triangle. The median value shown is calculated by taking the exponential of the average of the natural log of the data. The median peak roof drift predicted by the design procedure used for the archetype SC-CBFs is shown by a solid diamond. The median peak roof drift demand for the archetypes is 1.6% radians or less. Improvement in the prediction of the peak roof drift demand is needed for many of the archetype SC-CBFs and is the subject of ongoing research. The median peak story drift was 9%-34% higher than the median peak roof drift.

Two key assumptions of the behavior of SC-CBFs are that (a) rocking of the SC-CBF is primarily a first mode response and (b) that rocking of the SC-CBF and yielding of the PT steel limits the forces that can develop in the SC-CBF members. If the base overturning moment in the higher modes is significant, assumption (a) may be violated. Figure 9 compares modal overturning moment ratios calculated from time-history analysis results with design modal overturning moment ratios. The modal base overturning moments from time-history analysis were calculated by using the elastic mode shapes to decompose the restoring force vector at each time step into modal components. The result was then used to calculate modal base overturning moments. The modal base overturning moment ratio is the maximum of the absolute value of the base overturning moment for a mode divided by the sum of the maximum of the absolute value of the base overturning moment for each mode. The median value for the modal overturning moment ratio is shown with a solid bar. The median is calculated by taking the exponential of the average of the natural log of the data. The design modal overturning moment ratio for the first two modes is also shown. The plot of the modal overturning moment ratio shows that, as the height of the SC-CBFs increases, the assumption that the overturning moment response is primarily a first mode response is violated. This result raises some doubt about the effectiveness of the SC-CBF system studied herein as the height and aspect ratio increases.

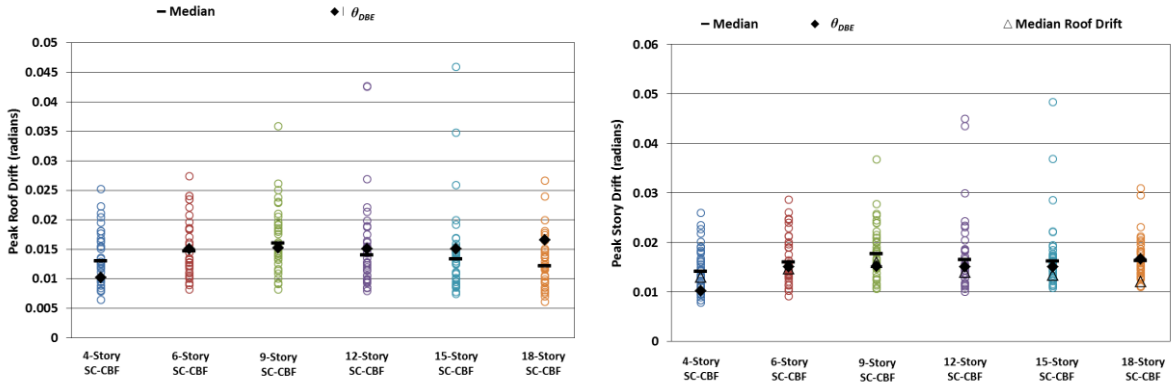

(a) (b)

Figure 8: (a) Peak roof demand and (b) peak story drift demand.

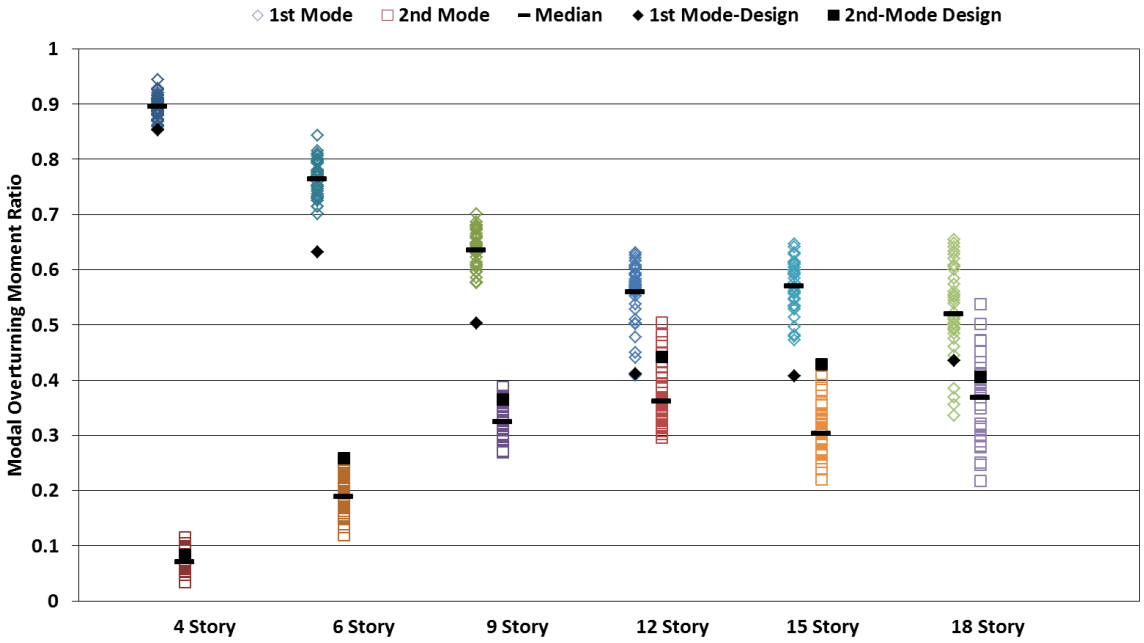

Figure 9: Modal overturning moment ratio from time-history analysis.

5 SUMMARY AND CONCLUSIONS

Steel SC-CBFs are a new type of seismic lateral force resisting system that reduces or eliminates the damage and residual drift often associated with conventional CBFs under the DBE. The SC-CBF system controls the member forces that can develop by assuming that the base overturning moment is a first mode response and then limits the base overturning moment by rocking of the SC-CBF and yielding of the PT steel. Six archetype SC-CBFs ranging from 4-stories to 18-stories were designed and subjected to design level earthquakes using time-history analysis. The median peak roof drift for the archetype SC-CBFs was 1.6% radians or less. The median peak story drift was 6% to 35% higher than the median peak roof drift. The difference between the median peak roof drift and median peak story drift generally increased with increasing aspect ratio. The first mode base overturning moment ratio generally decreased with an increase in aspect ratio while the second mode base overturning moment ratio generally increased with an increase in aspect ratio. Since the second mode base overturning moment ratio increases as the aspect ratio of the SC-CBF increases, this violates the assumed behavior and indicates that the SC-CBF member forces may not be as well controlled as thought. Methods of limiting higher mode response should be explored for SC-CBFs as the aspect ratio increases.

REFERENCES

[1] Roke, D.; Sause, R.; Ricles, J.M.; Seo, C.-Y.; and Lee, K.-S. (2006). "Self-Centering Seismic-Resistant Steel Concentrically-Braced Frames," Proceedings of the 8th U.S. National Conference on Earthquake Engineering, EERI, San Francisco, April 18-22.

[2] Roke, D.; Sause, R.; Ricles, J.M.; and Chancellor, N.B. (2010). "Damage-Free Seismic-Resistant Self-Centering Concentrically-Braced Frames." ATLSS Report 10-09, Lehigh University, Bethlehem, PA.

[3] Sause, R.; Ricles, J.M.; Roke, D.A.; Chancellor, N.B.; and Gonner, N.P. (2010a). "Seismic Performance of a Self-Centering Rocking Concentrically-Braced Frame." Proceedings of the 9th U.S. National and 10th Canadian Conference on Earthquake Engineering, EERI, Toronto, July 25-29.

[4] Sause, R.; Ricles, J.M.; Roke, D.A.; Chancellor, N.B.; and Gonner, N.P. (2010b). "Large-Scale Experimental Studies of Damage-Free Self-Centering Concentrically Braced Steel Frames Under Seismic Loading." NASCC Steel Conference/ASCE Structures Congress, Orlando, May 12-15.

[5] Hybrid Simulation: Theory, Implementation and Applications, Edited by Victor Saouma and Siva Mettupalayam, Francis and Taylor Publishers, London, England, 2008.

[6] Tremblay, R.; Poirier, L.-P.; Bouaanani, N.; Leclerc, M.; Rene, V.; Fronteddu, L.; and Rivest, S. (2008b). "Innovative Viscously Damped Rocking Braced Steel Frames," Proceedings of the 14th World Conference on Earthquake Engineering, Beijing, China, October 12-17.

[7] Eatherton, M.; Hajjar, J.; Ma, X.; Krawinkler, H.; and Deierlein, G. (2010a). "Seismic Design and Behavior of Steel Frames with Controlled Rocking – Part I: Concepts and Quasi-Static Subassembly Testing," Proceedings of the ASCE/SEI Structures Congress 2010, Orlando, FL, May 12-15.

[8] Eatherton, M.; Hajjar, J.; Deierlein, G.; Ma, X.; and Krawinkler, H. (2010b). "Hybrid Simulation Testing of a Controlled Rocking Steel Braced Frame System." Proceedings of the 9th U.S. National and 10th Canadian Conference on Earthquake Engineering, EERI, Toronto, July 25-29.

[9] Ma, X.; Eatherton, M.; Hajjar, J.; Krawinkler, H.; and Deierlein, G. (2010). "Seismic Design and Behavior of Steel Frames with Controlled Rocking – Part II: Large Scale Shake Table Testing and System Collapse Analysis," Proceedings of the ASCE/SEI Structures Congress 2010, Orlando, FL, May 12-15.

[10] Midorikawa, M.; Azuhata, T.; Ishihara, T.; and Wada, A. (2006). "Shaking Table Tests on Seismic Response of Steel Braced Frames with Column Uplift," Earthquake Engineering and Structural Dynamics, 35(14), pp 1767-1785.

[11] AISC (2005). Seismic Provisions for Structural Steel Buildings. American Institute of Steel Construction, Chicago, IL.

[12] ASCE (2005). Minimum Design Loads for Buildings and Other Structures, ASCE7-05. American Society of Civil Engineers (ASCE), Reston, VA.

[13] AISC (2005). Steel Construction Manual, 13th Edition. American Institute of Steel Construction, Chicago, IL.

[14] Seo, C.-Y. (2005). "Influence of Ground Motion Characteristics and Structural Parameters on Seismic Responses of SDOF Systems." Ph.D. Dissertation, Department of Civil and Environmental Engineering, Lehigh University, Bethlehem, PA.

[15] Mazzoni, S.; McKenna, F.; Scott, M.H.; Fenves, G.L.; et al. (2009). Open System for Earthquake Engineering Simulation (OpenSEES) User Command-Language Manual. Pacific Earthquake Engineering Research Center, University of California, Berkeley.

[16] Pacific Earthquake Engineering Research Center (PEER) (2011a). Ground motion database, http://peer.berkeley.edu/nga/earthquakes.html.

[17] Baker, J.W. (2011). "Conditional Mean Spectrum: Tool for Ground-Motion Selection," Journal of Structural Engineering, 137(3), pp 322-331.